

3D Visualization and Depth Analysis of Lung Nodule from CT Images

Nirmala Krishnamoorthi*¹, Venkateswaran N¹, Vinothkumar C¹

Sri Sivasubramaniya Nadar College of Engineering

Abstract

Lung nodules are abnormal growths in the lungs that can be non-cancerous or cancerous. NSCLC (non-small cell lung cancer) is one of the most common types of lung cancer, which amounts to about 80% of all lung cancer cases. It easily spreads to other parts of the body if it is not treated early. Hence, early detection and treatment is essential. In recent years, three-dimensional (3D) visualization techniques have transformed the medical field, particularly in the diagnosis and treatment of lung nodules. 3D visualization involves generating a 3D model of lung nodules using imaging data from computed tomography (CT) scans. The resultant 3D model provides a more accurate and detailed representation of the nodule's shape, size, and location. This can aid in treatment planning and surgical navigation. In addition, depth analysis helps to measure the nodule's depth and distance from other structures in the lung, providing crucial information for treatment decisions. Initially the CT images are preprocessed and then the region of interest is identified. The lung tissue is segmented followed by nodule extraction. The extracted nodules are then visualized, and the depth analysis is performed. In this work, nodules are extracted using U net architecture and 3D visualization is performed through volume rendering.

Keywords: *Lung nodule, 3D Visualization, U-net architecture, Depth analysis*

Introduction

CT lung nodule visualization in three dimensions (3D) offers more details than 2D imaging. For more accurate treatment planning, this provides doctors detailed information of the nodule's structure and spatial interactions. CT imaging produces high-resolution images of the inside of the body. These images are then assembled into 3D visualizations to provide a thorough view of the nodule from all directions [1]. During treatment or surgical planning, the clinicians use the 3D visualization of lung nodules which provide them with details of the like size, shape and its position. Additionally, 3D visualization also guides with other information like interaction of the nodule with nearby organs, nerves, or blood vessels, thereby helping the clinician to avoid damaging healthy tissue during surgical procedures and stop the nodule from spreading [2]. The nodule is visualized in multiple orientations namely axial, coronal, and sagittal planes. The comprehensive view of the nodule from different angles allows for a more detailed analysis of its characteristics in three dimensions.

Manual segmentation of lung nodules from CT images is a time-consuming, demands trained persons and may lead to human error [3]. On the other hand, the automated segmentation of lung nodules using deep learning techniques helps to overcome the above-mentioned challenges [4]. However, the performance of deep learning models depends on the quality and quantity of the training data. CT imaging datasets are often large and require significant resources for manual annotation. Additionally, the segmentation of lung nodules can be challenging due to the variability in size, shape, and location. The presented work aims to address these challenges by developing a deep learning

model for automated segmentation of lung nodules from CT images and generating 3D visualizations for depth analysis. The U-Net architecture, a widely used deep learning model for biomedical image segmentation is used for segmentation of lung nodule [5]. In recent years, deep learning techniques have gained popularity in the medical field for their ability to provide accurate and efficient analysis of medical images and shown promising results in the classification and tumor detection.

Ozdemir et al. (2019) [8] proposed a 3D probabilistic deep learning system for detecting and diagnosing lung cancer using low-dose CT scans. They have extracted the features using 3D convolutional neural network (CNN) and classified using Bayesian classifier. In addition to detection and diagnosis, Wang et al. (2008) [9] developed a display framework for visualizing real-time 3D lung tumor radiotherapy. Arlinda et al. (2019) [12] proposed a method for 3D reconstruction and visualization of lung cancer images using the marching cubes algorithm. Causey et al. (2020) [10] presented a system with 3D CNN with Spatial Pyramid Pooling (SPP) to extract discriminative features for lung cancer detection. The system was trained with large dataset to study the discriminative features for lung cancer. Cai Tao et al. (2020) [11] proposed a system that combines a region proposal network (RPN) with a Mask R-CNN for pulmonary nodule detection and segmentation. One study by Kadia et al. (2021) [6] included the U-Net architecture with residual and recurrent connections. Another study by Suryani et al. (2022) [7] proposed a method that used a combination of a deep fusion network and class activation mapping (CAM) to extract features from the chest X-ray image. Azad et al. (2020) [15] introduced the Bi-Directional ConvLSTM U-Net with Densely Connected Convolutions, which utilized bidirectional LSTM layers for processing temporal information in both forward and backward directions. Sahu et al. (2018) [16] provided a comprehensive overview of various image segmentation techniques, including thresholding, edge-based segmentation, region-based segmentation, and model-based segmentation. Then the authors discussed the efficiency of deep learning-based segmentation techniques. Another review by Cheng and Li (2021) [18] discussed the importance of image segmentation in digital image processing and its use in various applications, including medical imaging. From the early literature it is inferred that the deep learning-based lung segmentation provides promising results.

Methodology

The methodology of the presented work includes the dataset preparation, preprocessing of the dataset, segmentation of lung nodules, visualization of the lung nodules followed by volumetric analysis, *figure 1*. The dataset used is publicly available dataset, LUNA16, commonly used for the detection and diagnosis of lung cancer. It consists of 888 CT scans and an annotation file with 1186 nodules, annotated by four expert radiologists who marked the location and size of the nodules in each CT scan. The annotations also indicate whether the nodules are benign and malignant by categorizing into two classes, 0 and 1, for benign and malignant respectively.

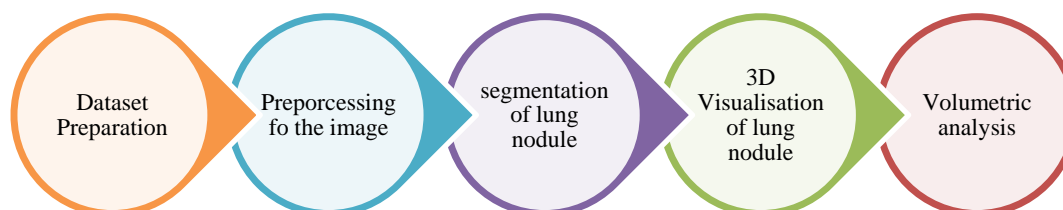


Figure 1. Methodology

The detailed process of the nodule segmentation is presented in *figure 2*. CT scans obtained are normalized to facilitate the detection of abnormalities and its characterization. It reduces the variability in image intensity and improves the contrast between nodules and surrounding tissue [23][24] and helps to reduce the computational complexity [25]. CT scans are typically affected by various sources of noise, such as photon noise, electronic noise, and structural noise [31]. Denoising helps to remove these types of noise and enhance the further process. The image is passed through a median filter with a kernel size of 7×7 to remove noise from the image. The lung nodule segmentation uses binary masks to identify the nodule from the lung tissue. Resizing operation is performed to ensure that all slices have the same size, 512×512 pixels, which is important for processing them in a batch. In this work the bicubic interpolation is used for resizing which preserves the image details. To the resized image the Contrast Limited Adaptive Histogram Equalization is used to enhance the contrast of an image. The contrast limit sets a threshold for the maximum allowed amplification in each tile. Any pixel intensity values that exceed this threshold are clipped or truncated to this maximum value. This helps to prevent over-enhancement of the image contrast and the introduction of unwanted artifacts. Lung nodule detection is a challenging task due to the low contrast, high variability, and small size of nodules. The k-means clustering algorithm is used to separate the pixels in the central area of the lung image into two groups. This is done to find a threshold value that separates the nodules from the background tissue [39]. The use of k-means clustering for thresholding in lung CT segmentation was seen to improve the accuracy and efficiency of lung nodule detection systems.

One common approach for lung nodule extraction is to use convolutional neural networks (CNNs), U-Net[29][30]. It consists of an encoder and decoder network that are connected by a series of skip connections. The encoder network learns to extract relevant features from the input image, while the decoder network uses these features to generate a segmentation map. The skip connections allow the decoder to recover detailed spatial information that was lost during the pooling operations of the encoder.

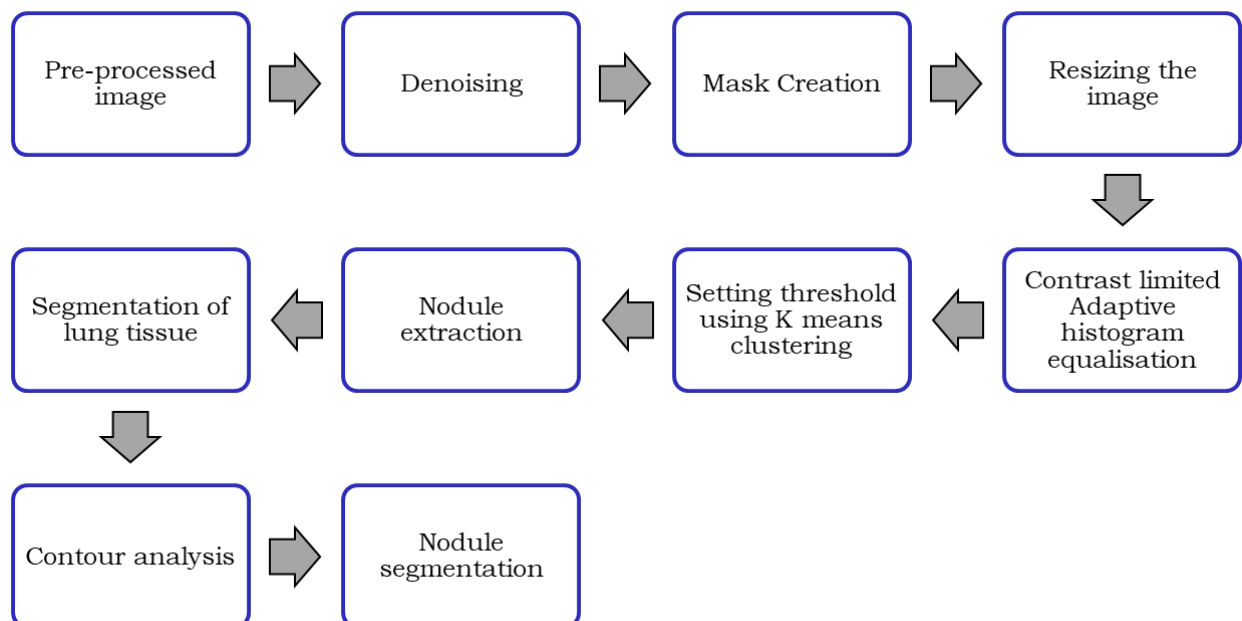


Figure 2. Process of Nodule Segmentation

Lung segmentation involves thresholding, specifically binary inverse thresholding, followed by erosion, to remove small regions of non-lung tissue that may have been included in the thresholded lung image and finally the dilation is performed to fill in any small holes or gaps that may be present in the lung image after the erosion operation. The three structuring elements used in the erosion and dilation operations have different sizes, allowing for different levels of smoothing and removal of non-lung tissue. Finally, a binary mask is created to isolate the lung regions using the filtered regions. Accurate segmentation of the lung Region of Interest ensures that nodules are correctly identified, and the false-positive rate is reduced.

The contours of the lung mask are identified and then, identification of the external contours of the lung mask is performed. This is achieved by iterating over all the contours and checking their hierarchy. The external contours are then dilated using a 4x4 kernel to expand them slightly. Following that, a series of morphological operations are applied to the contours to remove any holes and noise that may be present. This includes inverting the image, eroding it with a 7x7 kernel, inverting it again, dilating it with a 12x12 kernel, and finally eroding it with a 12x12 kernel. The final step is to apply a bitwise AND operation between the original normalized image and the segmented lung mask obtained in the previous steps. The resulting image is the final output of the lung segmentation process. The final steps involve refining the segmentation by removing any remaining noise or holes in the lung mask. This is achieved using additional morphological operations such as dilation and erosion.

Training a deep learning U-Net CNN for lung nodule segmentation can significantly improve accuracy compared to traditional methods. The U-Net architecture consists of an encoder and a decoder path, with a bottleneck layer in between, *figure 3*. The encoder path has two consecutive convolutional layers followed by a max pooling layer that reduces the spatial dimension of the feature maps. The first convolutional layer has 32 filters of size 3x3, and the second layer has 64 filters of size 3x3. The decoder path consists of two convolutional layers with the same filter sizes as the encoder path, followed by an up sampling layer that doubles the spatial dimensions of the feature maps. The bottleneck layer has two consecutive convolutional layers with 512 filters of size 3x3 each.

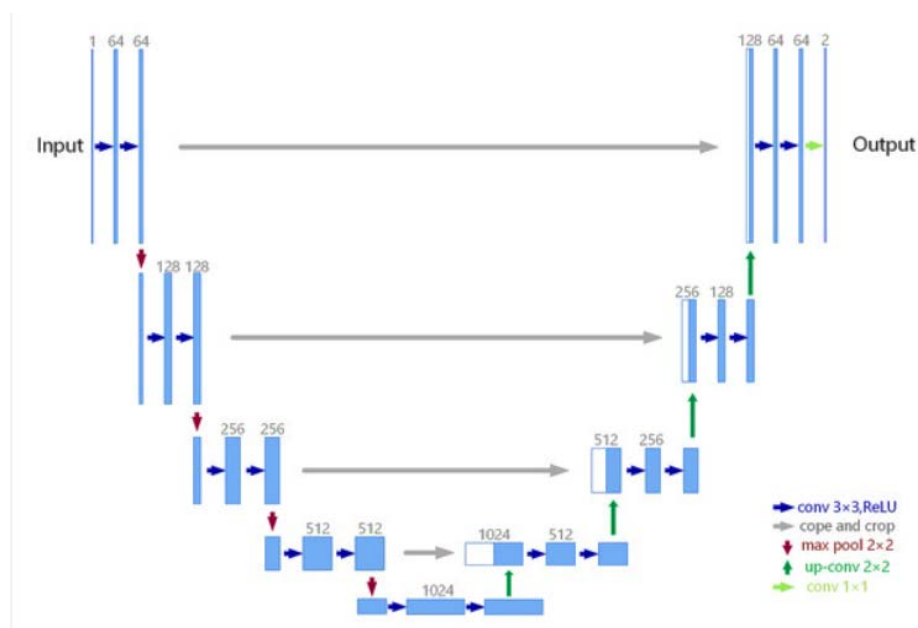


Figure 3 U-NET architecture [29]

The extracted nodules are 3D visualized to precisely pinpoint its location and determine its size and shape. The nodules are 3D visualized by rendering the volume using a transfer function that assigns distinct colors and opacities to the various components within the volume. Sphericity is a measure of how closely the nodule resembles a sphere. A low sphericity value indicates a more irregular shape, which can be suggestive of malignancy. Roundness is another parameter that measures how close the nodule resembles a circle, with values closer to 1 indicating a more circular shape. Surface area and compactness are also important parameters in volumetric analysis of lung nodules. Surface area is the total area of the nodule's surface, which can provide information on its growth rate and likelihood of malignancy. Compactness measures how tightly the nodule is packed, with higher values indicating a more aggressive growth pattern. Mean gray level, standard deviation of gray level, skewness, and kurtosis of gray level can provide information about the tissue characteristics of the nodule, which can help to distinguish between benign and malignant nodules. For example, higher values of skewness and kurtosis may suggest the presence of calcifications, which are often indicative of a benign nodule.

Result and Discussion

352 CT-Scan images from the Luna16 dataset were used. The obtained images are preprocessed, lung tissue is segmented and then the nodules are detected and extracted. The volume of the nodules is analyzed and 3 D visualization of the nodules are performed. *Table 1* shows the first stage which is nodule mask extraction and segmentation of the region of interest. Through a series of preprocessing and segmentation processes, generation of ground truth and lung region of interest is achieved. The performance analysis of the model is presented in *table 2*. *Figure 4* (a) and (b) shows the graph for Dice Coefficient and Loss Function of Model. A higher Dice coefficient indicates a better match between the predicted and ground truth masks. Loss Function of Model measures how well a model performs in terms of its ability to accurately predict an output given an input. *Figure 5* shows the Output of Segmentation and Nodule Extraction using 3D U-Net deep learning network. The U-Net used in this work consists of encoder path with two consecutive convolutional layers followed by bottleneck layer and at last a decoder path with consists of two convolutional layers with the same filter sizes as the encoder path, followed by an up-sampling layer that doubles the spatial dimensions of the feature maps. The output of the last convolutional layer in the decoder path is a binary mask which indicates the presence or absence of the target object in each pixel. The output has a sigmoid activation function to constrain the output to the range [0, 1]. *Figure 6* (a), (b) and (c) displays comparison of Ground Truth vs Prediction of Patient 1, Patient 2 and Patient 3 respectively.

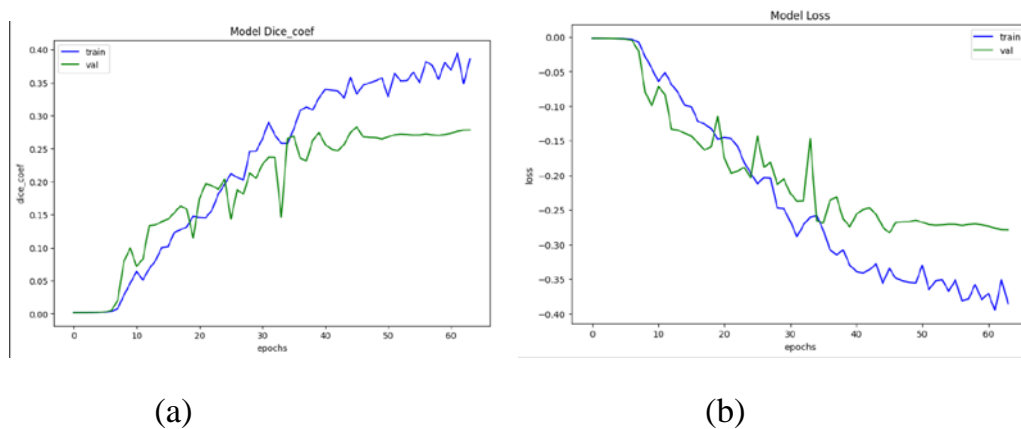
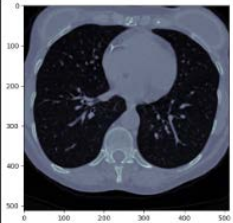
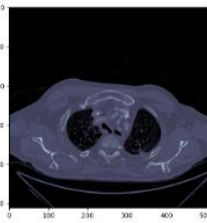
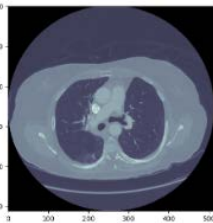
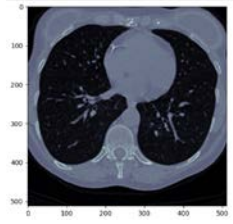
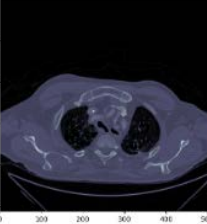
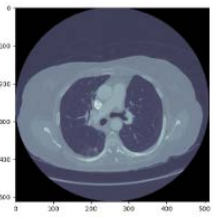
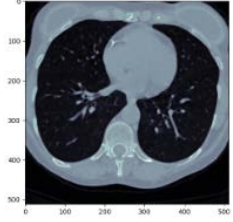
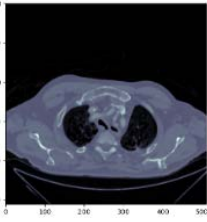
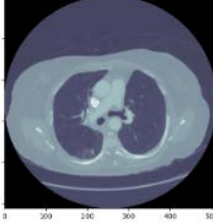
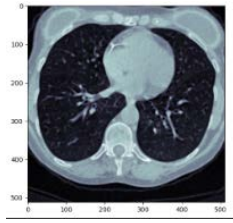
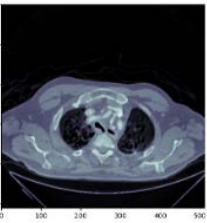

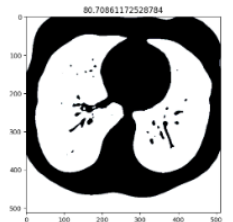


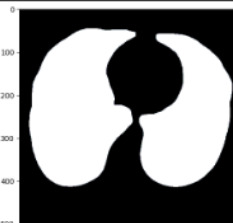




Figure 4. Performance analysis of the model

Table 1 Nodule Mask extraction and Segmentation

PROCESS	PATIENT 1	PATIENT 2	PATIENT 3
Test Images			
Preprocessed Dataset			
Applying Median Denoising			
Applying CLAHE			
Applying Inverse Binary Thresholding and K-means Clustering			
Final Mask for segmentation			

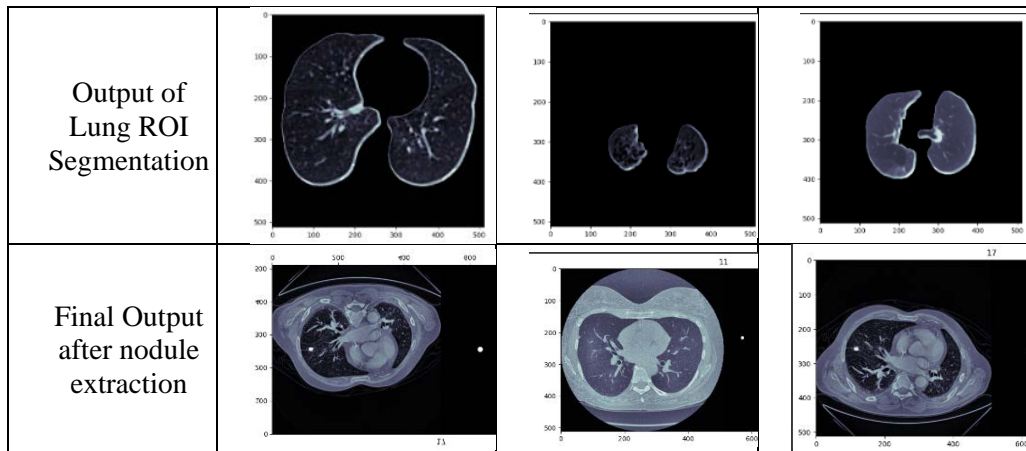


Table 2 Confusion Matrix Metrics

Measure	Value
Sensitivity	0.9183
Specificity	0.6632
Precision	0.8806
Negative Predictive Value	0.7500
False Positive Rate	0.3368
False Negative Rate	0.0817

Table 3. Volumetric Analysis

Parameter	Patient 1	Patient 2	Patient 3
Volume	127	125	216
Sphericity	0.4881	0.7575	1.4645
Roundness	0.0021	0.1005	0.0581
Surface Area in mm ²	268	125	148
Compactness	5.1379	0.9671	0.8059
Mean Gray Level	0.0071	1.1012	1.9029
STD Gray Level	0.00716	0.0010	0.0013
Skewness Gray Level	139.4991	952.92382	724.9128
Kurtosis Gray Level	19458.0233	908061.816	525496.629

Three-dimensional (3D) visualization of pulmonary nodules provides a more accurate and comprehensive understanding of nodule size, shape, location, and characteristics compared to

traditional two-dimensional (2D) methods. ITK-SNAP software is used for 3D visualization of the output segmented lung nodule. The 3D visualization of segmented lung and extracted nodule is shown in *Figure 7* and *Figure 8* respectively. Volumetric analysis of the extracted nodule is done using mathematical formulas and tabulated in *Table 3*. Mean gray level, standard deviation (STD) gray level, skewness gray level, and kurtosis gray level are commonly used statistical measures for image analysis in medical imaging, especially for tumor analysis.

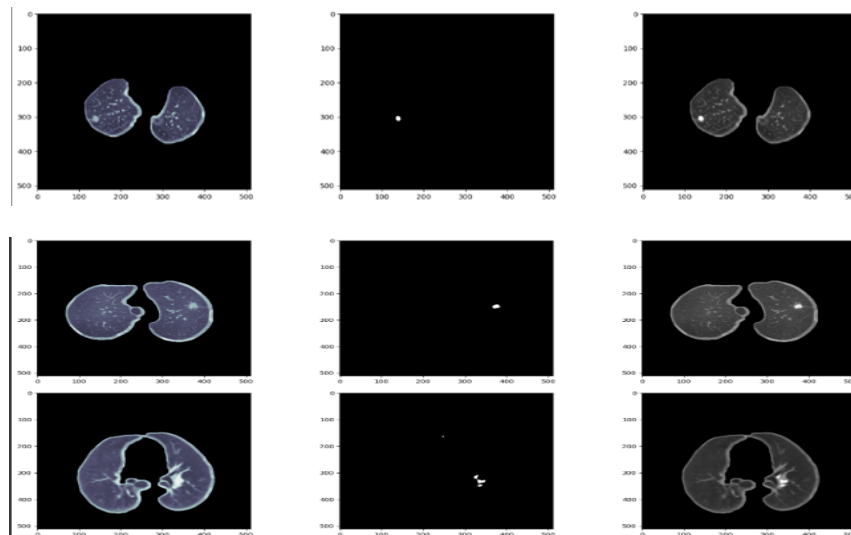


Figure 5 Output of Segmentation and Nodule Extraction

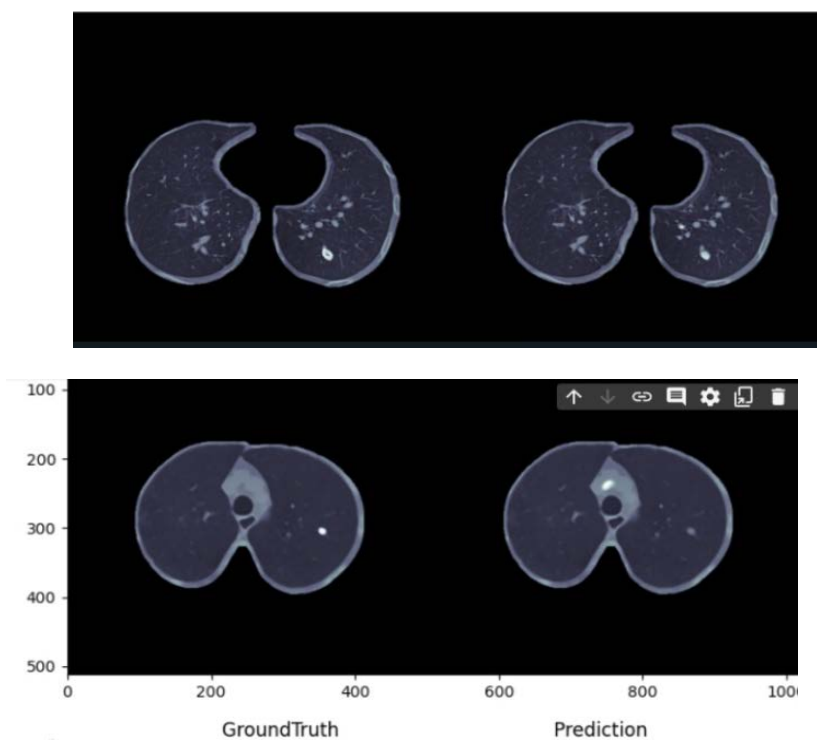


Figure 6 (a), (b) and (c) are Ground Truth vs Prediction of Patient 1, Patient 2 and Patient 3 respectively.

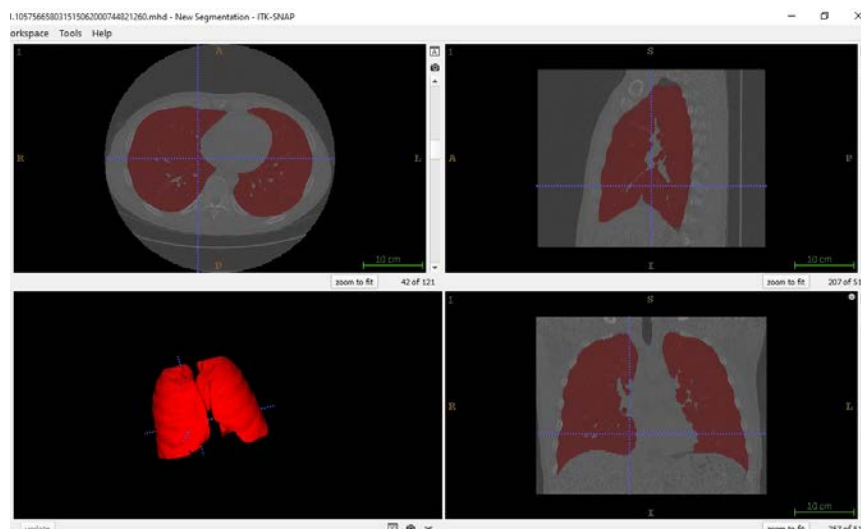


Figure 7. 3D Visualization of segmented Lung

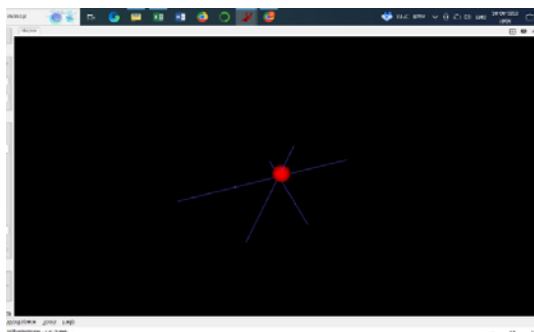


Figure 8.3D Visualization of Extracted Nodule

Conclusion

Medical imaging is essential for the diagnosis and management of many illnesses, especially those that affect the lungs. The CT images from the dataset are preprocessed and nodules are detected. The lung region is segmented from using the binary mask, generated using a sequence of morphological operations. The identified nodules are extracted using the U net architecture and further visualized using volume rendering. Volumetric analysis of the extracted nodules is performed to study the size, shape and position of the nodules. The U-Net Segmentation model has demonstrated remarkable performance in segmenting lungs, with a binary accuracy of 0.9977 and a dice coefficient of 0.2130. The model achieves this by identifying the regions of interest and extracting nodules from the annotations provided. While the predicted results have an 80% chance of providing the desired result, the remaining 20% possibility of false positives being detected can be attributed to structures within the lung that are like the structure of a nodule.

REFERENCES

1. S. S. Hwang, R. Naidich, and T. E. Rusinek, "Lung Nodule Detection on CT Scans," in *Imaging in Oncology*, 1st ed., New York: Springer Science Business Media, 2014, pp. 29-44.

2. D. W. K. Wong and S. M. Y. Law, "Three-Dimensional Imaging in Lung Cancer," *Journal of Thoracic Disease*, vol. 6, no. 12, pp. 1676-1686, 2014.
3. T. Cierniak, P. Bernasconi, M. Jerebko, and M. Tsirikika, "Deep learning for lung nodule detection: A review," *Computer Methods and Programs in Biomedicine*, vol. 196, pp. 105-121, 2020.
4. G. Litjens et al., "A survey on deep learning in medical image analysis," *Medical Image Analysis*, vol. 42, pp. 60-88, 2017.
5. O. Ronneberger, P. Fischer, and T. Brox, "U-Net: Convolutional networks for biomedical image segmentation," in *International Conference on Medical Image Computing and Computer-Assisted Intervention*, 2015, pp. 234-241.
6. Kadia, D. D., Zahangir, M., Burada, A. R., Nguyen, V., & Asari, V. K. (2021). R2U3D: Recurrent Residual 3D U-Net for Lung Segmentation. *IEEE Access*, 9, 174131-174142
7. Suryani, A. I., Chang, C. W., Feng, Y. F., Lin, T. K., Lin, C. W., Cheng, J. C., & Chang, C. Y. (2022). Lung Tumor Localization and Visualization in Chest X-Ray Images Using Deep Fusion Network and Class Activation Mapping. *IEEE Access*, 10, 1638-1650
8. Ozdemir, O., Russell, R. L., & Berlin, A. A. (2019). A 3D Probabilistic Deep Learning System for Detection and Diagnosis of Lung Cancer Using Low-Dose CT Scans. *IEEE Access*, 7, 96617-96627.
9. Wang, X., Chen, H., Gan, C., Lin, H., Dou, Q., Tsougenis, E., Huang, Q., & Cai, M. (2008). A Display Framework for Visualizing Real-Time 3D Lung Tumor Radiotherapy. *IEEE Access*, 26, 3475-3478.
10. Causey, J. L., Li, K., Chen, X., Dong, W., Walker, K., Qualls, J. A., Stubblefield, J., Moore, J. H., Guan, Y., & Huang, X. (2020). Spatial Pyramid Pooling with 3D Convolution Improves Lung Cancer Detection. *IEEE Access*, 8, 20941-20951.
11. Cai Tao, L., Dai, L. Y., & Huang, Y. (2020). Mask R-CNN-Based Detection and Segmentation for Pulmonary Nodule 3D Visualization Diagnosis. *IEEE Access*, 8, 154908-154918.
12. Arlinda, K., Mandaliana, M., Harsono, T., & Sigit, R. (2019). 3D Visualization and Reconstruction of Lung Cancer Images using Marching Cubes Algorithm. *IEEE Access*, 7, 136162-136173.
13. Sarker, P., Hossain, M. M., Shuvo, M. Z. H., & Hasan, S. (2018). Segmentation and Classification of Lung Tumor from 3D CT Image using K-means Clustering Algorithm. *IEEE Access*, 6, 15858-15870.
14. Wei, Q., Hu, Y., Mac Gregor, J. H., & Gelfand, G. (2016). Segmentation of Lung Lobes in Volumetric CT images for Surgical Planning of Treating Lung Cancer. *IEEE Access*, 4, 4628-4635.
15. Azad, R., Asadi-Aghbolaghi, M., Fathy, M., & Escalera, S. (2020). Bi-Directional ConvLSTM U-Net with Densely Connected Convolutions. *IEEE Access*, 8, 59446-59456.

16. Sahu, S., Sarma, H., & Bora, D. J. (2018). Image Segmentation and Its Different Techniques: An In-depth Analysis. *IEEE Access*, 6, 16612-16629. doi.org/10.1109/ACCESS.2018.2800130
17. Yuanyuan, W., Yi, G., & Chunran, Y. (2019). Automatic Detection and Segmentation of Lung Nodule on CT Images. *IEEE Access*, 7, 50108-50119. doi.org/10.1109/ACCESS.2019.2918566
18. Cheng, Y., & Li, B. (2021). Image Segmentation Technology and Its Application in Digital Image Processing. *IEEE Access*, 9, 20092-20106. doi.org/10.1109/ACCESS.2021.3060418
19. Sammouda, R. (2017). Segmentation and Analysis of CT Chest Images for Early Lung Cancer Detection. *IEEE Access*, 5, 13618-13628. doi.org/10.1109/ACCESS.2017.2715184
20. Cui, H., Wang, X., & Feng, D. (2012). Automated Localization and Segmentation of Lung Tumor from PET-CT Thorax Volumes Based on Image Feature Analysis. *IEEE Access*, 1, 618-625. doi.org/10.1109/ACCESS.2013.2242906
21. Shaziya, H., Shyamala, K., & Zaheer, R. (2018). Automatic Lung Segmentation on Thoracic CT Scans using U-Net Convolutional Network. *IEEE Access*, 6, 69016-69024. doi.org/10.1109/ACCESS.2018.2887924
22. Zhou, Y., Ming, C., Zhang, M., Wang, T., Yan, F., & Xie, C. (2020). Automatic Segmentation of Lung Nodules using improved U-Net Network. *IEEE Access*, 8, 148230-148241. doi.org/10.1109/ACCESS.2020.3012082
23. Ardila, D., Kiraly, A. P., Bharadwaj, S., Choi, B., Reicher, J. J., Peng, L., ... & Shetty, S. (2019). End-to-end lung cancer screening with three-dimensional deep learning on low-dose chest computed tomography. *Nature medicine*, 25(6), 954-961.
24. Zhou, Y., Rajchl, M., & Yuan, J. (2018). Lung nodule detection via deep reinforcement learning with sample efficient trust region method. In *International Conference on Medical Image Computing and Computer-Assisted Intervention* (pp. 274-282). Springer, Cham.
25. Ghavami, N., Barati, M., & Naghizadeh, R. (2019). A review of preprocessing techniques in MRI brain tumor segmentation. *Computer methods and programs in biomedicine*, 170, 1-17.
26. A. Aldape-Pérez, et al., "Medical Image Preprocessing Techniques for Clinical Applications: A Review," *Journal of Medical Systems*, vol. 44, no. 5, p. 93, 2020. doi: 10.1007/s10916-020-01593-5.
27. T. Cierniak, P. Bernasconi, M. Jerebko, and M. Tsikrika, "Deep learning for lung nodule detection: A review," *Computer Methods and Programs in Biomedicine*, vol. 196, pp. 105-121, 2020.
28. G. Litjens et al., "A survey on deep learning in medical image analysis," *Medical Image Analysis*, vol. 42, pp. 60-88, 2017.
29. O. Ronneberger, P. Fischer, and T. Brox, "U-Net: Convolutional networks for biomedical image segmentation," in *International Conference on Medical Image Computing and Computer-Assisted Intervention*, 2015, pp. 234-241.

30. H. Li, Z. Li, and L. Pu, "Lung nodule segmentation based on 3D U-Net with multiple scales inputs," in 2018 IEEE 15th International Symposium on Biomedical Imaging (ISBI 2018), 2018, pp. 441-444.
31. Pham DL, Xu C, Prince JL. Current methods in medical image segmentation. Annual review of biomedical engineering. 2000;2(1):315-37.
32. Senthilkumar, P. (2012). Image segmentation using binary masks. International Journal of Computer Science and Network Security, 12(11), 1-5
33. Chen, C. M., Chang, R. F., & Huang, Y. L. (2008). Adaptive neighbor slice-based lung nodule segmentation on chest CT images. Journal of Medical Imaging and Radiation Oncology, 52(1), 60-68.
34. Tsehay, Y., Addisu, G., & Eyasu, A. (2019). Segmentation of lung nodules in CT images using enhanced convolutional neural networks. Journal of digital imaging, 32(6), 983-993.
35. Wu, X., Kim, H., & Balagurunathan, Y. (2012). Comparison of 3D adaptive filtering and traditional filtering for nodule detection in low-dose CT. Medical Physics, 39(5), 2793-2801.
36. Ibragimov, B., Xing, L., & Akhundov, J. (2014). Segmentation of lungs and lung tumors from low dose CT scans using a new contrast minimization algorithm. PloS one, 9(3), e91006.
37. L. A. Gomes de Sá, A. C. Patrocínio, and J. J. Silva Cunha Jr, "An approach for contrast enhancement of medical images using CLAHE and entropy-based thresholding," in Proc. IEEE Int. Conf. on Image Processing, 2015, pp. 3869-3873.
38. Chen, S., Zhang, Z., Zhou, Y., & Feng, J. (2017). Lung nodule detection via deep convolutional neural networks based on 3D CT images. Neurocomputing, 267, 378-390. doi: 10.1016/j.neucom.2017.06.015
39. Shen, W., Zhou, M., Yang, F., Yu, D., Dong, D., Yang, C., ... & Tian, J. (2017). Multi-crop convolutional neural networks for lung nodule malignancy suspiciousness classification. Radiology, 284(2), 566-576.
40. Jacobs C, van Rikxoort EM, Murphy K, et al. Automatic segmentation of pulmonary nodules in thoracic computed tomography images by combining local intensity structure and texture features. Med Image Anal. 2014;18(5):877-892. doi:10.1016/j.media.2014.03.008
41. Kim JH, Lee JG, Park YS, Lee JH, Lee CT. An efficient approach to segment lung nodule based on morphology and convolutional neural networks. Sci Rep. 2019;9(1):9631. Published 2019 Jul 3. doi:10.1038/s41598-019-45736-5
42. Huo, Y., Chen, H., Li, Y., Li, Q., Xie, H., Zhang, X., ... & Liang, Z. (2018). Lung nodule segmentation using 3D deep dense multi-scale convolutional neural networks. Medical physics, 45(6), 2878-2889.
43. Gao, J., Wang, C., Zhou, X., Zhang, Z., & Hu, Y. (2018). A deep learning-based approach to classification of CT scans for lung nodules. IEEE Transactions on Medical Imaging, 37(6), 1522-1531.

44. Christodoulidis, S., Anthimopoulos, M., Ebner, L., Christe, A., Mougiakakou, S. (2018). Multi-source transfer learning with convolutional neural networks for lung pattern analysis. *IEEE Journal of Biomedical and Health Informatics*, 22(3), 736-745.